LES-simulation of heat transfer in a turbulent pipe flow with lead coolant at different Reynolds numbers

K.M. Sergeenko[1], V.M. Goloviznin[2], V.Yu. Glotov[2]

[1]JSC NIKIET, Moscow, Russia, [2]IBRAE, Moscow, Russia

E-mail contact of main author: km.sergeenko@nikiet.ru

Abstract. Study of turbulent pipe flows is extremely important because of its wide range of applications. In the past decades, many fundamental theoretical and experimental studies on the wall-bounded flows have been performed: in the pipe, flat channel and boundary layer flow geometries. However, the internal fluid dynamics in these regions still far from being understood. Numerical simulation offers an opportunity to get detailed information on the flow structure, which is difficult to obtain experimentally.
In this paper, the numerical simulation of turbulent heat transfer in a circular pipe was performed in a wide range of Reynolds numbers using nonparametric MILES-method CABARET on grids with an incomplete resolution of the turbulence spectrum, as well as with the use of the STAR-CCM+ code in a LES-approximation. The calculation results were compared with the DNS calculations by other authors found in literature, as well as with the RANS-calculations performed in the STAR-CCM+ code. The simulation showed a satisfactory accuracy in determining an average, rms and integral characteristics of the flow, and revealed drawbacks in the existing model relations describing the local properties of turbulence. The authors have proposed a wall-bounded thermal function, which might be implemented in the RANS-approximations.

Key Words: pipe flow, turbulent heat transfer, liquid-metal coolant, LES

1. Introduction

High coolant temperature is one of the distinctive features of fast neutron reactors of a new generation under design. This feature dictates the need for an increased accuracy in determination of the heat transfer coefficient which defines the heat-transfer surface temperature. Current approaches to the calculation of engineering thermal-hydraulic problems are largely based on the use of RANS turbulence models. However, use of RANS approximation requires turbulence to be “quasistationary” (the representative timescale is much smaller than the task’s period). Relatively stable large-scale unsteady coherent structures may affect greatly the turbulence parameters. The characteristics of these structures depend on the given geometry and the boundary conditions and cannot be therefore described as part of semiempirical models [1]. The findings show that RANS models do not take into account the specific nature of heat transfer in liquid metal coolants, which leads to a divergence between calculation and experimental data. The error in such calculations amounts to 25% [2, 3]. This may requires the use of eddy-resolving turbulence models, e.g. LES. The LES application experience indicates to a high accuracy of calculations for not only average but also local flow characteristics even when elementary algebraic subgrid models of turbulence are used. Monotonic numerical methods make it possible not to use “subgrid” turbulence modeling since this work is done by numerical dissipation (MILES) [4-6].
This study deals with numerical modeling of turbulent heat transfer in conditions of a lead coolant flow in a circular pipe in a broad range of Reynolds numbers (Re = 5300, 11700, 19000 and 37700) based on CABARET-STAGES, a CABARET-scheme code [7], and STAR-CCM+ code, in LES (WALE) and RANS (k-e realizable) approximations [8]. With subgrid turbulence scales filtered implicitly as the result of a CABARET-based nonlinear flow correction [9], one may classify it as a MILES method. This methodology does not

contain any setup parameters.The results of the study have been verified against the DNS calculations performed based on a high-order spectral element method (Nek5000, 2013) [10]. The above Reynolds numbers were selected because exactly these numbers were used to obtain the DNS calculation data.

2. Governing equations and grid model

The modeling coolant is a Newtonian incompressible fluid with constant properties described by equations [11]:

$$\begin{cases} div(\mathbf{u}) = 0 \\ \dfrac{\partial u_i}{\partial t} + div(u_i \mathbf{u}) + \dfrac{1}{\rho}\nabla_i P = \nu \Delta u_i, \quad i = 1..3 \\ \dfrac{\partial T}{\partial t} + div(T\mathbf{u}) = a\Delta T \end{cases} \tag{1}$$

where ρ : density; P : pressure; T : temperature; $\mathbf{u}$: velocity vector; ν : kinematic viscosity; a : capacity.

The computational domain is formed by a tube of the radius $R = 5 \cdot 10^{-3}$ m and the length L with the symmetry axis along the Z axis in Cartesian coordinates. The fluid is driven by the pressure gradient which is regulated dynamically from the condition of the mass flow conservation along the tube. The adhesion conditions and a constant heat flux of $q_w \approx 10^5 W/m^2$ are specified for the side surfaces. Periodic boundary conditions with the given mass-averaged inlet temperature of $T_b = 773\ ^\circ K$ are set on the tube ends.

Hexagonal grids were used for the calculations (*Fig. 1*, Table I).

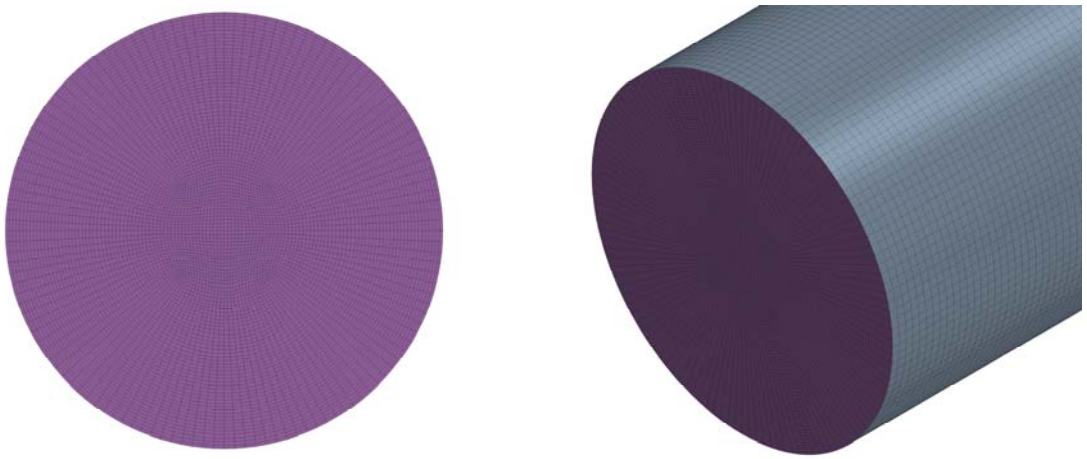

FIG. 1. Grid model fragments (Re=5300)

TABLE I: GRID MODEL PARAMETERS

Re	**L/R**	$\mathbf{N_{cell}}$	$\mathbf{N_\varphi}$	N_z	$\Delta \mathbf{r}^+_{min}$	$\Delta \mathbf{R\theta}^+_{max}$	Δ^+_{center}	$\Delta \mathbf{z}^+$
5300	20	2.98×10^6	128	440	3.0	8.8	3.1-3.5	8.1
11700	10	5.22×10^6	200	320	3.0	11.2	4.4-5.0	11.2
19000	10	19.52×10^6	320	500	3.0	10.8	4.4-5.0	11.0
37700	15	44.16×10^6	624	1000	3.0	10.1	12.9	15.0

3. Results

3.1. Integral flow characteristics

One of the major flow characteristics is friction factor (C_f) and Nusselt number (Nu). Friction factor (*Fig. 2a,* Table II) is defined by the relation:

$$C_f = \Delta P / L \cdot 4R / \rho V_b^2 , \quad (2)$$

where ΔP is the pressure difference in the region of interest, *Pa*; and V_b is the mass-averaged fluid velocity, *m/s*. For $5 \cdot 10^3 < \mathrm{Re} < 10^5$ the Blasius formula is valid:

$$C_f = 0.3164 / \sqrt[4]{\mathrm{Re}} . \quad (3)$$

The Nusselt number (*Fig. 2b,* Table III) is defined by the relation:

$$Nu = q_w / (T_w - T_b) \cdot 2R / \lambda , \quad (4)$$

where T_w is the wall temperature, *°K*; and λ is the conductivity, *W/(m°K)*.

Two well-known dependences are used for the turbulent stabilized heat transfer calculation. The Lyon formula obtained by an approximation of the numerical solution in a circular tube under the condition of $\mathrm{Pr} < 0.1$ and $\mathrm{Pr}_t = 1$:

$$Nu = 7 + 0.025 \cdot Pe^{0.8} . \quad (5)$$

The second dependence was obtained by Subbotin (IPPE) [12] based on an experimental data:

$$Nu = 5 + 0.025 \cdot Pe^{0.8} . \quad (6)$$

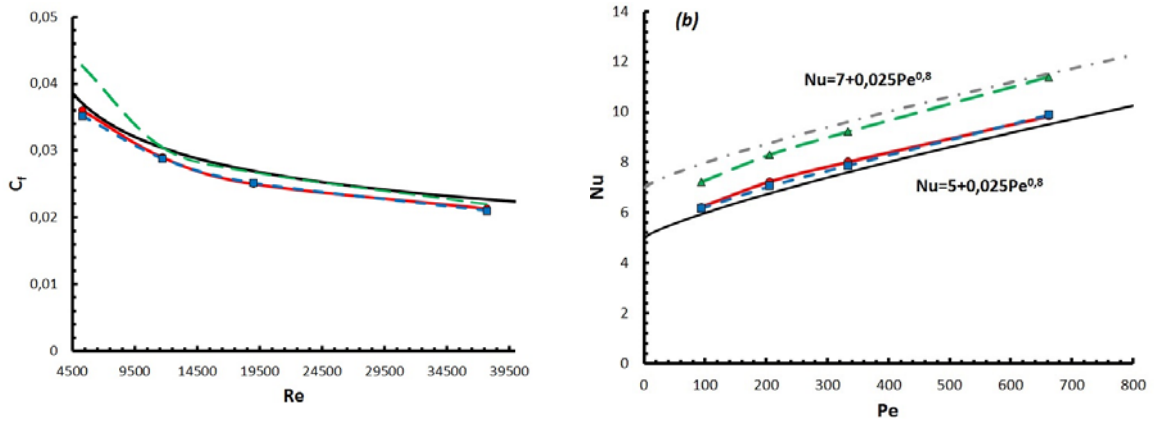

FIG. 2. a - friction factor; b - Nusselt number;
—, CABARET; - - -, LES (WALE); - - -, RANS (k-e real.)

Calculated Nusselt number is approximated by expression:

$$Nu = 5.4 + 0.025 \cdot Pe^{0.8} . \quad (7)$$

TABLE II: FRICTION FACTOR

Re	Blasius formula	CABARET	LES (WALE)	RANS (k-e realizable)
5300	0.0370	0.0355 (-4.0%)	0.0352 (-5.1%)	0.0427 (+15.4%)
11700	0.0304	0.0289 (-5.0%)	0.0288 (-5.2%)	0.0305 (+0.24%)
19000	0.0269	0.0250 (-7.1%)	0.0251 (-6.7%)	0.0268 (-0.3%)
37700	0.0227	0.0213 (-6.1%)	0.0210 (-7.5%)	0.0220 (-3.3%)

TABLE III: NUSSELT NUMBER

Re	Subbotin formula	CABARET	LES (WALE)	RANS (k-e realizable)
5300	5.94	6.22 (+4.8%)	6.18 (+4.0%)	7.22 (+21.5%)
11700	6.77	7.23 (+6.8%)	7.06 (+4.2%)	8.31 (+22.7%)
19000	7.61	8.02 (+5.4%)	7.89 (+3.7%)	9.22 (+21.1%)
37700	9.52	9.83 (+3.3%)	9.90 (+4.0%)	11.39 (+19.7%)

3.2. Average flow characteristics

Other important characteristics of the turbulent boundary layer are axial velocity profile (*Fig. 3a*) and temperature profile (*Fig. 3b*). The theoretical velocity distribution has the form [13]:

$$u_z^+\left(y^+\right)=\begin{cases}u_z^+\left(y^+\right)=y^+, & y^+<5\\ 1/\kappa\cdot\ln\left(y^+\right)+C, & y^+>30\end{cases}, \tag{8}$$

where $\kappa\approx 0.41$ is Karman constant; $C\approx 5.5$. The temperature distribution has the form [13]:

$$T^+=\begin{cases}y^+\,\mathrm{Pr}, & y^+\,\mathrm{Pr}<1\\ 1.87\ln\left(y^+\,\mathrm{Pr}+1\right)+0.065y^+\,\mathrm{Pr}-0.36, & y^+\,\mathrm{Pr}=1-11.7,\\ 2.5\ln\left(y^+\,\mathrm{Pr}\right)-1, & y^+\,\mathrm{Pr}>11.7\end{cases} \tag{9}$$

where $T^+=\left(T_w-T\right)/T_\tau$, $T_\tau=q_w/\left(\rho C_V u_\tau\right)$ is temperature scale ("friction temperature"). The temperature distribution in the channel's central region is parabolic.

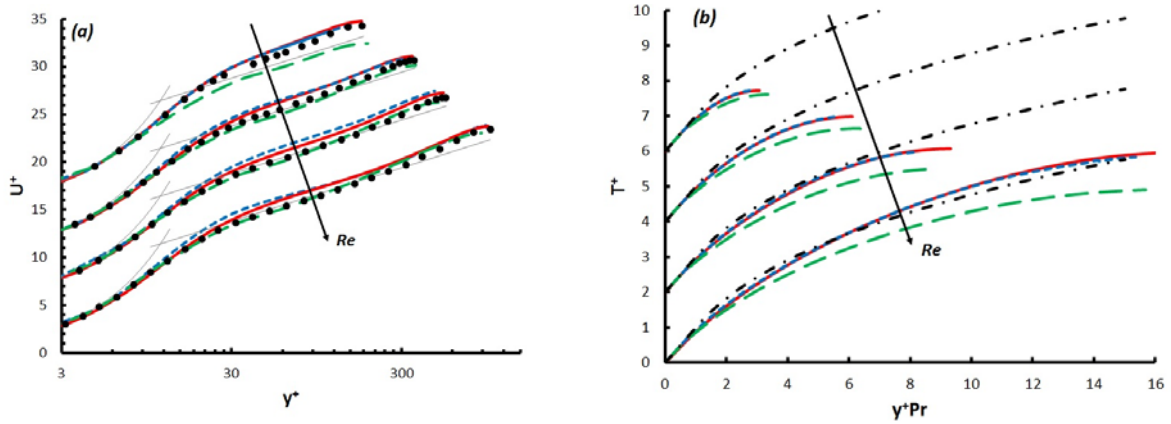

FIG. 3. a – average velocity profile. b – average temperature profile;
● , DNS [10]*; — , (8); — · — , (9); — , CABARET; - - - , LES (WALE); - - - , RANS (k-e real.)*

3.3. Turbulent kinetic energy

Relation for turbulent kinetic energy (TKE):

$$dk/dt=P^k+\varepsilon^k+\Pi^k+D^k+T^k, \tag{10}$$

where $k=\left(\left\langle u_r^{'2}\right\rangle+\left\langle u_\theta^{'2}\right\rangle+\left\langle u_z^{'2}\right\rangle\right)/2$: TKE; $P^k=-\left\langle u_i^{'}u_j^{'}\right\rangle\partial\left\langle u_i\right\rangle/\partial x_j$: production; $\varepsilon^k=-\nu\cdot\left\langle\partial u_i^{'}/\partial x_j\cdot\partial u_i^{'}/\partial x_j\right\rangle$: viscous dissipation; $\Pi^k=-1/\rho\cdot\partial\left\langle pu_i^{'}\right\rangle/\partial x_i$: pressure-related diffusion; $D^k=\nu/2\cdot\partial^2\left\langle u_i^{'}u_i^{'}\right\rangle/\partial x_j^2$: viscous diffusion and $T^k=-1/2\cdot\partial\left\langle u_i^{'}u_i^{'}u_j^{'}\right\rangle/\partial x_j$: turbulent velocity related diffusion. Fig. 4 shows profiles of the turbulent kinetic energy k^+, and Fig. 5 shows its budgets: generation P^k and dissipation $\Delta^k=\varepsilon^k+\Pi^k+D^k+T^k$.

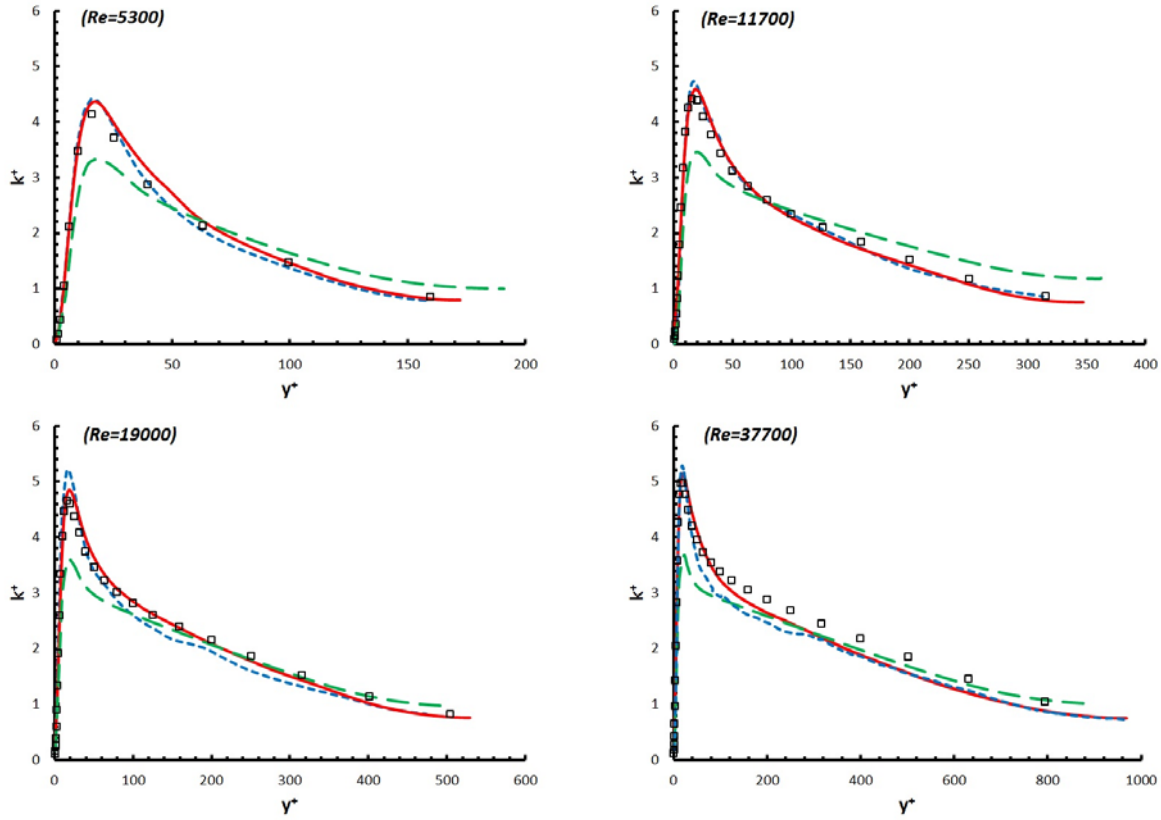

FIG. 4. Turbulent kinetic energy normalized by u_τ^2 *;*
▫ *, DNS* [10]*;* — *, CABARET;* - - - *, LES (WALE);* - - - *, RANS (k-e real.).*

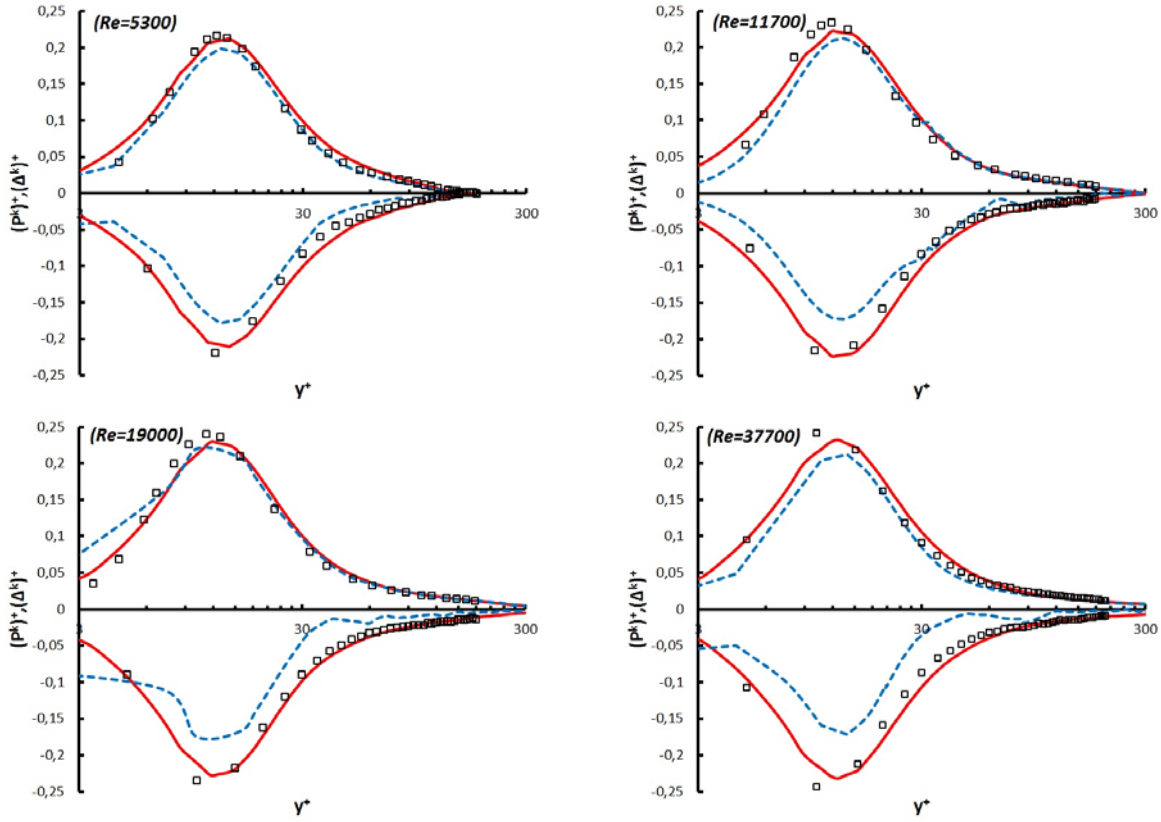

FIG. 5. Kinetic turbulence energy budget normalized by u_τ^4/ν *;*
▫ *, DNS* [10]*;* — *, CABARET;* - - - *, LES (WALE)*

3.4. Temperature energy

Relation for the temperature energy is:

$$d\left\langle T'^2\right\rangle / dt = P^T + \varepsilon^T + D^T + T^T, \tag{11}$$

where $P^T = -2\left\langle u_i' T'\right\rangle \partial\left\langle T\right\rangle / \partial x_i$: production; $\varepsilon^T = -2 \cdot a \cdot \left\langle \partial T' / \partial x_i \cdot \partial T' / \partial x_i \right\rangle$: capacity dissipation; $D^T = a \cdot \partial^2 \left\langle T'^2 \right\rangle / \partial x_i^2$: molecular diffusion; and $T^T = -\partial\left\langle u_i' T'^2 \right\rangle / \partial x_i$: turbulent velocity-related diffusion. Fig. 6 shows profiles of RMS of temperature $\sqrt{\left\langle T'^2\right\rangle}$, and the energy budget: production P^T and dissipation $\Delta^T = \varepsilon^T + D^T + T^T$.

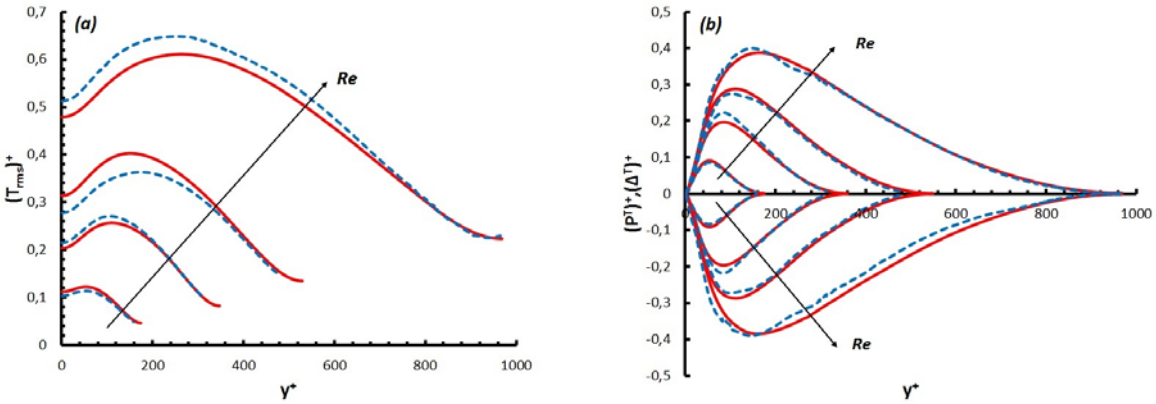

FIG. 6. a – RMS temperature normalized by T_τ, b – temperature energy budget normalized by $T_\tau^2 u_\tau^2 / a$; —, CABARET; - - -, LES (WALE)

3.5. Turbulent transport coefficients

Turbulent Prandtl number (Pr_t), representing the relation of turbulent viscosity (ν_t) to turbulent capacity (a_t), are encountered in semiempirical turbulence theories which assume that turbulent stresses are proportional to the averaged velocity gradient $\left(\left\langle u_r' u_z'\right\rangle = -\nu_t \partial\left\langle u_z\right\rangle / \partial r\right)$, and agitation-caused heat fluxes are proportional to the averaged temperature gradient ($\left\langle u_r' T'\right\rangle = -a_t \partial\left\langle T\right\rangle / \partial r$). It is also assumed that turbulent transport coefficients are scalars (in a general case, with anisotropy taken into account, they are second-order tensor quantities).

It is important to know the average number $\left\langle \mathrm{Pr}_t \right\rangle$ when calculating the heat transfer characteristics with the use of semiempirical models in which the turbulent Prandtl number is assumed to be constant across the flow. For coolants with Pr<1, for instance, a variation $\left\langle \mathrm{Pr}_t \right\rangle$ in the range (1-3) with Reynolds numbers being Re≈10^5, may lead to Nusselt number values differing by more than 100% [14]. The data from a LES-approximation calculation (Fig. 7) may be used for the calibration of different semiempirical turbulence models. Fig. 8 presents respective RANS model results.

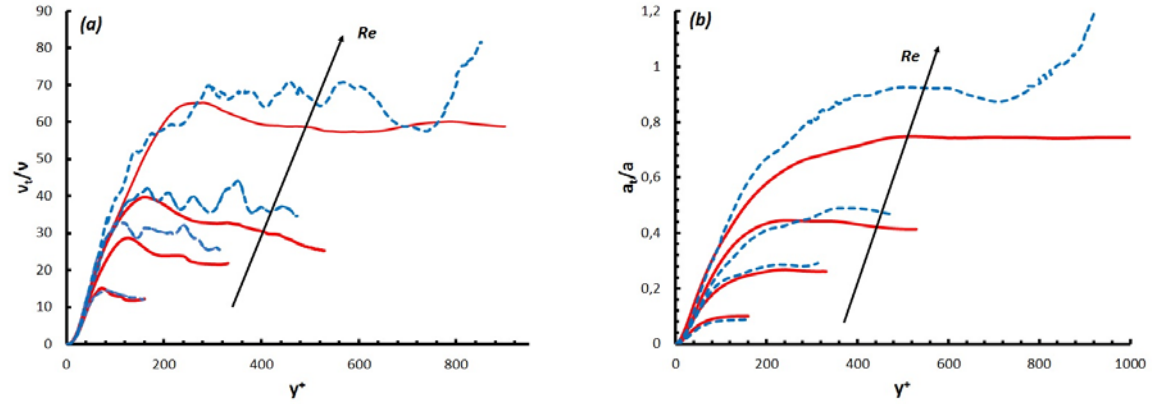

FIG. 7. a – turbulent viscosity normalized by ν; b – turbulent capacity normalized by a; — , CABARET; - - - , LES (WALE).

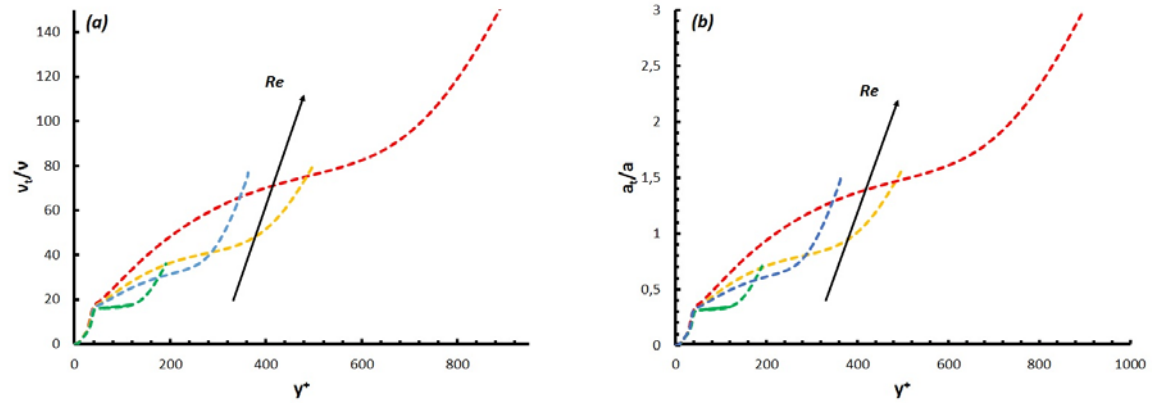

FIG. 8. a – turbulent viscosity normalized by ν; b – turbulent capacity normalized by a; RANS

The turbulent Prandtl numbers are shown in Fig. 9. Different integral estimates of the form as follows can be used to determine average turbulent transport coefficient values

$$\langle X \rangle = \int_V f \cdot X \cdot dV \Big/ \int_V f \cdot dV \,, \tag{12}$$

where X is the quantity of interest, and f is the weight function. The following weight function values were assumed in this study (see Table IV):

TABLE IV: VALUES OF WEIGHT FUNCTIONS

X	Pr_t	ν_t / ν	a_t / a
f	$q_t = \langle u_r' T' \rangle$	$f_\nu = \partial \langle u_z \rangle / \partial r$	$f_a = \partial \langle T \rangle / \partial r$

TABLE V: INTEGRAL ESTIMATES OF TURBULENT TRANSPORT COEFFICIENTS

Re	CABARET			LES (WALE)			RANS (k-e realizable)	
	$\langle \nu_t / \nu \rangle$	$\langle a_t / a \rangle$	$\langle \mathrm{Pr}_t \rangle$	$\langle \nu_t / \nu \rangle$	$\langle a_t / a \rangle$	$\langle \mathrm{Pr}_t \rangle$	$\langle \nu_t / \nu \rangle$	$\langle a_t / a \rangle$
5300	2.46	0.049	3.01	2.61	0.042	2.74	3.3	0.19
11700	5.23	0.151	2.22	6.12	0.114	2.28	6.63	0.345
19000	9.44	0.268	1.82	13.27	0.260	2.03	8.79	0.470
37700	13.46	0.473	1.38	20.68	0.627	1.65	15.1	0.809

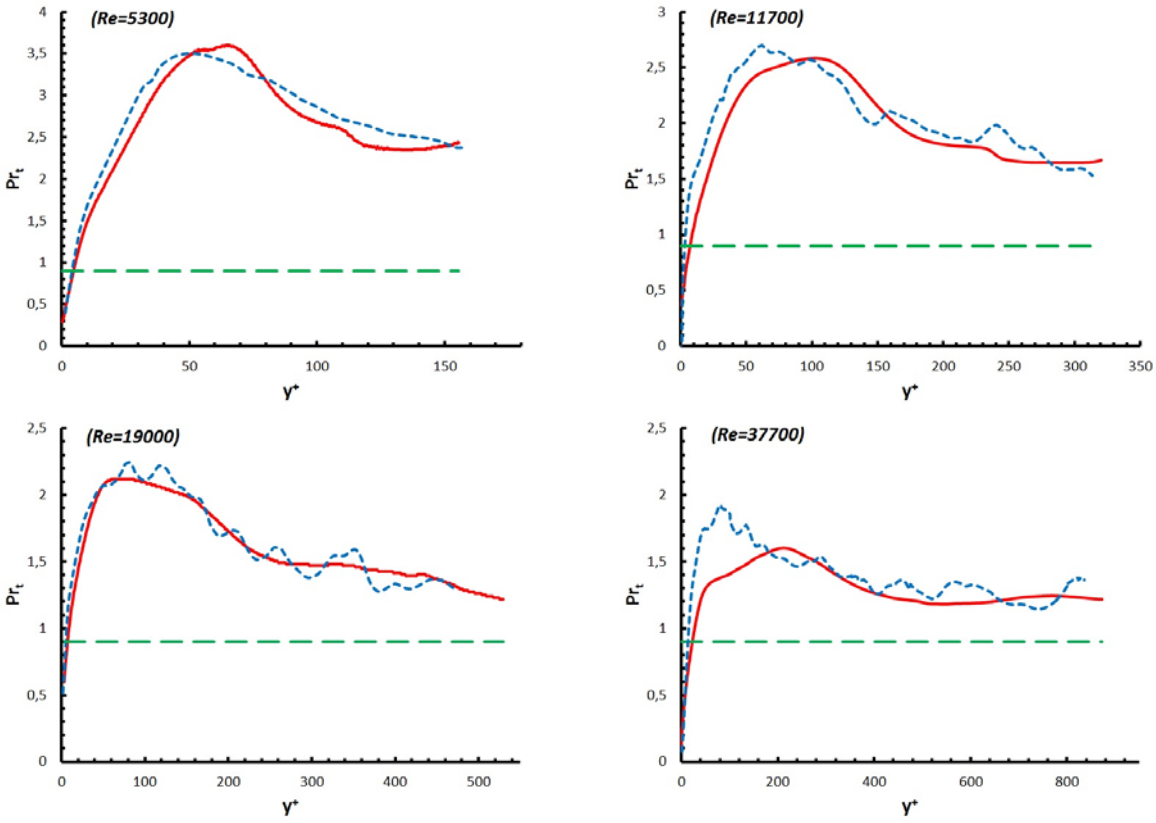

FIG. 9. Turbulent Prandtl number; —, CABARET; - - -, LES (WALE); - - -, RANS (k-e real.)

It can be seen form Tables II and III that, except Re=5300, RANS approximation agrees well in terms of the HRC values, while the heat transfer coefficient is determined with a 20% deviation. It can be also suggested that the overestimated heat transfer coefficient value has been caused by the invalid value of the turbulent Prandtl number used in the RANS approximation. Thus, the turbulent Prandtl number value is 1.5 to 3 times as great as that given in the RANS model in use (Table V). However, the values of the "effective" turbulent Prandtl number approach unity as the Reynolds number increases (Fig. 10), while the heat transfer coefficient value remains at the 20% deviation level.

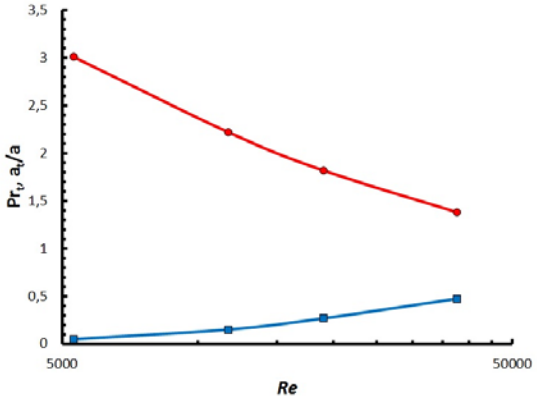

FIG.10. —, $\langle \mathrm{Pr}_t \rangle$; —, $\langle a_t / a \rangle$.

The heat flux transferred through turbulent velocity and temperature oscillations in the fluid flow is expressed by the expression (Lyon integral):

$$\frac{1}{Nu} = 2\int_0^1 \left[\left(\int_0^R urdr \right)^2 \Big/ \left(1 + \mathrm{Pr}/\mathrm{Pr}_t \cdot \nu_t/\nu\right) \right] dR \qquad (13)$$

Therefore, apart from the local value of the turbulent Prandtl number, the heat flux is defined by the local turbulent viscosity value. RANS approximation leads to a major deviation in the local turbulent viscosity values (Fig. 8a), with its effective value remaining the same (Table V) and the friction factor being determined correctly.

3.6. Wall thermal function

The wall thermal function connects the amount of the heat transferred to the heat-transfer surface to the gradient of temperature in the channel adjoining the wall. So, knowing the distribution T^+, it is possible to construct the thermal function for the modeled coolant. Thus, by approximating the calculated values T^+ by the relation:

$$T^+ = A \cdot Ln(\mathrm{Pr} \cdot y^+ + B) + C \cdot \mathrm{Pr} \cdot y^+ + D\,, \qquad (14)$$

where *A=3.15; B=3.0; C=0.04;* and *D=-3.46,* we obtain a wall thermal function fit for being integrated into the RANS turbulence model.

4. Conclusions

This study deals with modeling of a turbulent lead coolant flow in a circular pipe with LES approximation in a broad range of Reynolds numbers. A good agreement (with an accuracy of ~5%) has been shown with DNS calculations and reference data for all major flow characteristics. Coefficients of turbulent transport have been studied. The findings can be used as a benchmark for the calibration of different semiempirical turbulence models.

The study has showed that for considered type of flow, Bussinesk approximation is valid and value of turbulent Prandtl number is tend to be unity while Reynolds number is increasing. Reason of errors in RANS approximation is based on incorrect simulation of local value of turbulent viscosity. So, there are 2 options in the turbulent heat transfer problem solution in RANS approximations:

- modification of the turbulent Prandtl number depending on the turbulent model in use;
- use of the assumption that turbulent viscosity and turbulent capacity are equal with a further turbulence model setting for an increased accuracy in the turbulent viscosity value determination.

In addition, it needs to be understood that the first option is a simpler way but its evolution leads to an incorrect description of the turbulent heat transfer process.

Acknowledgements We would like to thank A. Solovjev, V. Nikonorov, I. Ilkin, A. Tutukin, D. Svetlichnyy and direction of ours institutes for their help in present work.

References

[1] GARBARUK, A.V., “Turbulence modeling in calculations of complex flows: training guide”, A.V. Garbaruk, M.Kh. Strelets, M.L. Shur – SPb: Polytechnic University Publ., 2012. – 88 p.

[2] GROTZBACH, G., et al., “Validation of turbulence models in the computer code FLUTAN for free hot sodium jet in different buoyancy flow regimes”, Forschugszentrum Karlsruhe GmbH, Karlsruhe, FZKA 6600, 2003, 34 p.

[3] WOLTERS J., “Benchmark Activity on the TEFLU Sodium Jet Experiment”, Forschungszentrum Jülich GmbH, FZJ, 2002, 66 p.

[4] ORAN, E.S., et al. “Numerical Simulation of reactive flow”, 2001: CUP.

[5] GRINSTEIN, F.F., et al., “Implicit Large Eddy Simulation”, 2007: CUP.

[6] BORIS, J.P., et al., “New insights into large eddy simulation”, Fluid Dynamics Research, 1992, **10**(4-6): p. 199-228.

[7] GOLOVIZNIN, V.M., et al., “New algorithms of computational fluid dynamics for multiprocessor computer systems”, 2013, Moscow: Moscow University Publ., 472.

[8] USER GUIDE. Star-CCM+ Version 10.02 – CD-adapco, 2015

[9] GOLOVIZNIN, V.M., et al., “Nonlinear CABARET correction”, Matematichskoye modelirovaniye, 1998. **10**(12): pp. 107-123.

[10] KHOURY, G.K.E., et al., “Direct Numerical Simulation of Turbulent Pipe Flow at Moderately High Reynolds Numbers”, Flow Turbulence Combust (2013), 2013. 91: p. 475-495.

[11] TANNEHILL J.C., et al., “Computational Fluid Mechanics and Heat Transfer: in 2 v. V. 2”, 1990, Moscow, Mir Publ., 392 p.

[12] SUBBOTIN, V.I., et al., “Heat exchange in conditions of a liquid metal flow in tubes”, Inzhenerno-fizicheskiy zhurnal, 1963. **6**(4): pp. 16-20.

[13] KIRILLOV, P.L., et al., “Reference book on thermal-hydraulic calculations (Nuclear reactors, heat exchangers, steam generators)”, 1990, Moscow: Energoatomizdat. 360 p.

[14] GROSHEV, A.I., V.I. SLOBODCHUK, “Influence of turbulent Prandtl number on heat transfer in tubes”, FEI-1463. Obninsk: IPPE, 1983. – 22 pp.